Transient Analysis of Coaxial Cables Considering Skin Effect*

R. L. WIGINGTON† AND N. S. NAHMAN‡, ASSOCIATE MEMBER, IRE

Summary—**A transient analysis of coaxial cables is made by considering the skin effect of the center conductor as the distorting element. Generalized curves are presented by which the response of any length of coaxial cable can be predicted if one point on the attenuation vs frequency curve is known. An experimental check on the analysis is made by comparing measurements and prediction of the responses of several different coaxial cables.**

Introduction

IN A STUDY of oscilloscope systems for use in observing voltage waveforms of the duration of a few millimicroseconds (1 mμs$=10^{-9}$ sec), the problem of the distortion of waveforms by the high frequency loss of coaxial cable was encountered. Elementary consideration of the problem indicated a degradation of fast rise times (1 mμs or less) due to greater attenuation of the high-frequency components of the signal.

In polyethylene dielectric coaxial cables, the conductance loss is extremely small. Polyethylene has a dissipation factor of 0.0031 at 3000 mc[1] and less at lower frequencies. Likewise, in air dielectric cables the conductance loss is even less. Therefore, the major portion of high-frequency loss could not be blamed on leakage conductance. The other source of loss in coaxial cable is the series resistance of the center conductor. For analysis the skin effect of the outer conductor was considered to be lumped with the skin effect of the center conductor increasing it slightly. Using empirical data to evaluate the skin effect constant achieves this directly. Ordinary analysis of transmission lines ignore this resistance as being negligible. However, at frequencies at which the skin effect of conductors becomes significant, the analysis must include its effects, both as series resistance and inductance.

In this analysis, a transmission line is treated as a four-pole network. With the aid of an approximation which is good at high frequencies, an analysis including skin effect and neglecting dielectric effects can be made. All calculations are in mks units.

Possible Applications

Before proceeding with the analytical details of the problem, a few words about the engineering applications would be indicative of the role which skin effect distortion in coaxial cables may play in contemplated and future systems using fast transients.

The origination of this problem was in the design of an oscilloscope system for observing very fast rise times, 1 mμs or less. In triggered oscilloscope systems a signal delay path (usually a simulated line or a coaxial cable) is necessary to allow time for the trigger circuits to detect the pulse to be observed and to start the sweep. The delay of this path is 50 mμs or longer in present systems. As shown in this paper, the distortion in this amount of coaxial cable is very serious for millimicrosecond transients. Therefore, along with the other limitations of oscilloscope systems (such as rise time of the signal amplifiers, writing speed, and vertical sensibility), the distortion due to the signal delay cable must be considered. Perhaps a knowledge of the form of this distortion will enable the extension of the range of oscilloscope systems which are limited by the signal delay distortion.

If preserving the rise times in fast pulse circuits is in any way critical to the proper operation of the circuitry, one must begin to consider the skin effect distortion in 10-mc prf circuits for long cable runs, and in 100-mc prf circuits, the distortion would be troublesome even in short cable lengths. The practice of using special small size coaxial cable to conserve space results in greater attenuation per unit length than for larger cable of the same characteristic impedance, and thus, also makes the skin effect distortion greater.

Another example of a problem in which the analysis may be very useful is in the analysis of regenerative pulse generators, a circuit which is essentially a loop consisting of an amplifier and a delay circuit.[2] For practical, high rep-rate pulse generation, the delay circuit is usually a coaxial cable. The pulse shape obtained is a composite of the characteristics of the cable and of the amplifier.

In short, for any electronic circuit application using coaxial cables as transmission media to provide either time delay or transmission of millimicrosecond pulses, the effects of skin effect distortion must be considered.

Analysis

For a transmission line of length, l, terminated in its characteristic impedance, Z_0, and with propagation constant, γ, the following relation exists between input (E_1) and the output (E_2) voltages as functions of complex frequency:[3]

* Original manuscript received by the IRE, August 20, 1956; revised manuscript received, October 18, 1956.

† Natl. Security Agency, Washington, D. C.
‡ Univ. of Kansas, Lawrence, Kan. Formerly with Natl. Security Agency, Washington, D. C.

[1] "Reference Data for Radio Engineers," Federal Telephone and Radio Corp., 3rd ed., p. 51.

[2] C. C. Cutler, "The regenerative pulse generator," PROC. IRE, vol. 43, pp. 140–148; February, 1955.

[3] The complex variable is the Laplace Transform variable p. Eqs. (1) and (2) comprise the Laplace Transform equations of the system differential equations.

$$E_2 = e^{-\gamma l}E_1 \tag{1}$$

where in general

$$\gamma = \sqrt{(R + pL)(G + pC)} \tag{2a}$$

$$Z_0 = \sqrt{\frac{R + pL}{G + pC}}. \tag{2b}$$

For high frequencies (skin depth small with respect to conductor radius), the skin effect impedance of a round wire is:[4]

$$Z_s = K\sqrt{p} \tag{3a}$$

and

$$K = \frac{1}{2\pi r}\sqrt{\frac{\mu}{\sigma}} \tag{3b}$$

where r is conductor radius, μ is the permeability and σ is the conductivity of the wire.

At high frequencies the series resistance of a wire is expressed by the skin effect equation. Since an increase in inductance is also caused by skin effect, it is treated as an impedance rather than as a resistance. Therefore, replacing R in (2) by Z_s and neglecting dielectric leakage ($G=0$), (2) becomes

$$\gamma = \sqrt{(K\sqrt{p} + pL)pC} \tag{4a}$$

$$Z_0 = \sqrt{\frac{K\sqrt{p} + pL}{pC}}. \tag{4b}$$

The transfer function of a length of line is then:

$$\frac{E_2}{E_1} = e^{-\gamma l} = e^{-l\sqrt{p^2LC + pCK\sqrt{p}}}. \tag{5}$$

The inverse Laplace Transform of the transfer function (5) is the impulse response of the section of line. For simplification, the following approximation was made. Expanding the square root in the exponent of (5) by the binomial expansion, one obtains

$$\begin{aligned}\gamma(p) &= (p^2LC + p^{3/2}CK)^{1/2} \\ &= p\sqrt{LC} + \frac{Kp^{1/2}}{2}\sqrt{\frac{C}{L}} + \frac{1}{2}\sum_{n=2}^{\infty}(-1)^{n-1} \\ &\quad \cdot\left(\frac{1\cdot 3\cdot\cdots\cdot(2n-3)}{2^{n-1}n!}\right)\frac{K^n}{L^{n-1}}\sqrt{\frac{C}{L}}\,p^{1-n/2}.\end{aligned} \tag{6}$$

The first term of (6) is the delay term and the remaining terms describe the waveform distortion. The series is an alternating convergent series (for $p^2LC > p^{3/2}CK$). Approximating it by the second term of (6), the $p^{1/2}$ term, results in an error less than the next term, the p^0 term. The ratio of these two terms will be used as a measure of validity of applying this approximation to specific examples.

$$A \equiv \left|\frac{p^0 \text{ term}}{p^{1/2} \text{ term}}\right| = \left|\frac{\frac{K^2}{8L}\sqrt{\frac{C}{L}}}{\frac{Kp^{1/2}}{2}\sqrt{\frac{C}{L}}}\right| = \left|\frac{K}{4Lp^{1/2}}\right|$$

$$= \frac{K}{4L\sqrt{2\pi f}}. \tag{7}$$

Using the first two terms of (6) in (5) and letting $R_0 = \sqrt{L/C}$, $T = \sqrt{LC}$, results in

$$\frac{E_2}{E_1} = e^{-l(pT + (K/2R_0)p^{1/2})}. \tag{8}$$

The exp $(-ltp)$ is simply a delay term so that the inverse transform of (8) is the inverse transform of exp $(-lkp^{1/2}/2R_0)$ delayed an amount lT. The latter exponential is a common transform and is listed in ordinary Laplace Transform tables.[5] Its inverse giving the impulse response is:

$$\begin{aligned} g(t) &= \alpha x^{-3/2}e^{-\beta/x} && x \geqq 0 \\ &= 0 && x < 0 \end{aligned} \tag{9}$$

where

$$\alpha = \frac{lK}{4R_0\sqrt{\pi}},\quad \beta = \left(\frac{lK}{4R_0}\right)^2,\quad \text{and } x = t - Tl.$$

Of greater utility in studying the distortion of fast rise times by skin effect are the step response and the response to a linear rise. The step response can be obtained by finding the inverse transform of $1/p$ times the transfer function. As before, the transform $1/p$ exp $(-lkp^{1/2}/2R_0)$ is listed in tables.[5] Therefore in terms of x and β as defined above, the step response is:

$$\begin{aligned} h(t) &= \operatorname{cerf}\sqrt{\frac{\beta}{x}} && x \geqq 0 \\ &= 0 && x < 0. \end{aligned} \tag{10}$$

cerf (y) is the "complementary error function of y."

The linear rise referred to previously is defined specifically as the following, and it will be referred to as a ramp input.

$$\begin{aligned} F(t) &= 0 && t < 0 \\ &= t/a && 0 \leqq t \leqq a \\ &= 1 && t > a. \end{aligned}$$

The response to $F(t)$, called $f(t)$, is given by the convolution of $F(t)$ with the impulse response of the line, $g(t)$.

$$f(t) = \int_0^t F(t - \tau)g(\tau)d\tau.$$

This integral reduces to the following special cases:

[4] S. Ramo and J. R. Whinnery, "Fields and Waves in Modern Radio," John Wiley and Sons, Inc., New York, N. Y.; 1944.

[5] S. Goldman, "Transformation Calculus and Electrical Transients," Prentice-Hall, Inc., New York, N. Y., p. 423; 1949.

Case I: $0 < t \leqq Tl$ $f(t) = 0$ since $g(\tau) = 0$ for $\tau < Tl$

Case II: $Tl \leqq t \leqq Tl + a$

$$f(t) = \int_0^x \left(\frac{x-\tau}{a}\right) \tau^{-3/2} e^{-\beta/\tau} d\tau \qquad x = t - Tl$$

Case III: $t > Tl + a$

$$f(t) = \int_0^{x-a} \tau^{-3/2} e^{-\beta/\tau} d\tau + \int_{x-a}^{x} \left(\frac{x-\tau}{a}\right) \tau^{-3/2} e^{-\beta/\tau} d\tau, \qquad x = t - Tl.$$

Note that Case II is contained in Case III providing that the integrands are limited to positive values of τ only for Case II.

Considering Case III only and evaluating with the aid of the identity derived in Appendix I, one obtains

$$f(t) = \operatorname{cerf} \sqrt{\frac{\beta}{x-a}} + \frac{x}{a}\left(\operatorname{cerf} \sqrt{\frac{\beta}{x}} - \operatorname{cerf} \sqrt{\frac{\beta}{x-a}}\right) - \frac{1}{a}\int_{x-a}^{x} \tau\alpha\tau^{-3/2} e^{-\beta/\tau} d\tau. \tag{11}$$

Integrating the last term of (11) by parts one obtains

$$\frac{1}{a}\int_{x-a}^{x} \tau\alpha\tau^{-3/2} e^{-\beta/\tau} d\tau = \frac{x}{a} \operatorname{cerf} \sqrt{\frac{\beta}{x}} - \frac{x-a}{a} \operatorname{cerf} \sqrt{\frac{\beta}{x-a}} - \frac{1}{a}\int_{x-a}^{x} \operatorname{cerf} \sqrt{\frac{\beta}{\tau}}\, d\tau. \tag{12}$$

Observing that the first two terms of (12) cancel the corresponding terms of (11), the function $f(t)$ is simply,

$$f(t) = \frac{1}{a}\int_{x-a}^{x} \operatorname{cerf} \sqrt{\frac{\beta}{\tau}}\, d\tau \qquad \begin{matrix} x \geqq 0 \\ x = t - Tl \end{matrix} \tag{13}$$

with the understanding that for $x < a$ the lower limit is zero.

As verification, one may note that the limit of the ramp response as "a" approaches zero is simply the step response. Also, as x gets large, the function approaches unity; physical interpretation of the function required that this be true.

Evaluation of Constants

Using the first two terms of (6), the propagation constant is approximately

$$\gamma(p) = \rho T + \frac{K}{2R_0} p^{1/2}$$

$$\gamma(j\omega) = \frac{K}{2R_0}\sqrt{\frac{\omega}{2}} + j\left(\omega T + \frac{K}{2R_0}\sqrt{\frac{\omega}{2}}\right).$$

The real part of $\gamma(j\omega)$ is the attenuation constant of the transmission line, for the purposes of the analysis, called $C(f)$.

$$C(f) = \frac{K\sqrt{\pi f}}{2R_0} \text{ nepers/meter.} \tag{14}$$

Any coaxial cable whose attenuation constant obeys the above law will have a straight line relation of slope one-half between the logarithm of the attenuation constant and the logarithm of the frequency. The majority of types of coaxial cable have very nearly this characteristic (see Fig. 1). The ratio of $C(f)$ to $\sqrt{f}$ from (14) is therefore a constant for each type of cable and can be calculated from the attenuation characteristic of the cable.

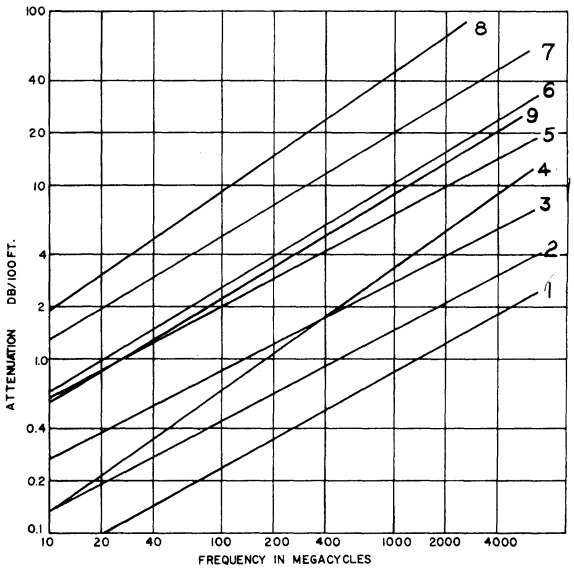

1) Styroflex $1\frac{5}{8}$ inches
2) Styroflex $\frac{7}{8}$ inch
3) Styroflex $\frac{1}{2}$ inch
4) RG—19, 20/u
5) RG—63/u
6) General Radio—874A2
7) RG—58 A/u
8) RG—38, 39, 40/u
9) RG—8/u

References:
1), 2), 3)—Brochure of Phelps-Dodge Copper Products Corp.
4), 5), 7), 8), 9)—"Reference Data for Radio Engineers," Federal Telephone and Radio Corp., 3rd ed.
6)—Catalog *N*, General Radio Co.

Fig. 1—Attenuation vs frequency characteristics for common coaxial cables.

In this way, the value of K, and subsequently of β, can be evaluated for each case as follows:

$$\beta = \left(\frac{lK}{4R_0}\right)^2 = \left(\frac{l}{4R_0}\,\frac{2R_0C(f_0)}{\sqrt{\pi f_0}}\right)^2 = \left(\frac{lC(f_0)}{2\sqrt{\pi f_0}}\right)^2 \tag{15}$$

where f_0 is the frequency chosen to evaluate β. For convenience in calculation let $l = T_l/T$ where T_l is the time length of the cable and $T = \sqrt{LC}$ is the delay per unit length.

$$\beta = \left(\frac{T_lC(f_0)}{2T\sqrt{\pi f_0}}\right)^2. \tag{16}$$

Resistive Termination

The analysis assumes that the transmission line is terminated in its characteristic impedance which is given in (4b). However, in the ordinary circuit, a purely resistive termination of value $R_0=\sqrt{L/C}$ would be used. To see at what frequencies R_0 would be a good approximation for Z_0, the following comparison of actual Z_0 with R_0 is made.

From (4b)

$$Z_0 = \sqrt{\frac{pL+K\sqrt{p}}{pC}} = \left(R_0^2+\frac{K}{C\sqrt{p}}\right)^{1/2}$$
$$= R_0+\frac{K}{2R_0C\sqrt{p}}-\frac{K^2}{8R_0^3C^3p}+\cdots\cdots. \quad (17)$$

The fractional deviation of Z_0 from R_0 as a function of p is less than the second term of (17) divided by R_0. The smallness of the magnitude of this fraction indicates the closeness of approximation.

$$\left|\frac{Z_0(p)-R_0}{R_0}\right| < \left|\frac{K}{4R_0^2C\sqrt{p}}\right| = \frac{K}{4R_0^2C\sqrt{2\pi f}}. \quad (18)$$

Since $R_0^2C=L$ then (18) is the same as (7). Thus, A, the validity constant calculated previously is also an expression of the departure of Z_0 from R_0.

Generalization of Theory

In order to present curves with which any transient problem involving skin effect distortion of rise times could be solved, the theory is generalized. First, the assumption is made that any rising function can be approximated sufficiently closely for engineering analysis by a series of a few straight line segments. The response to any function can then be obtained from the sum of the responses to the ramp functions used for approximation. A generalized ramp response is then the function to be plotted.

Recalling from the analysis the three basic functions,

Impulse response $\equiv g(t)$

$$= g(x+Tl) = \sqrt{\frac{\beta}{\pi}}\,x^{-3/2}e^{-\beta/x} \quad (9)$$

Step response $\equiv f(t) = f(x+Tl) = \operatorname{cerf}\sqrt{\frac{\beta}{x}}$ (10)

Ramp response $\equiv h(t)$

$$= h(x+Tl) = \frac{1}{a}\int_{x-a}^{x}\operatorname{cerf}\sqrt{\frac{\beta}{\tau}}\,d\tau \quad (13)$$

$x \geqq 0$, all cases,

the problem is to generalize them so that β, the constant which is determined by the specific case, does not appear in the functions, but only in the scales to which the responses are plotted.

As the first step, the transformation $x=\beta\rho$ is used in (9). The resulting function of ρ is[6]

$$g_0(\rho) = \frac{\rho^{-3/2}e^{-1/\rho}}{\beta\sqrt{\pi}} \qquad \rho \geqq 0 \quad (19)$$

or

$$\beta g_0(\rho) = \frac{\rho^{-3/2}e^{-1/\rho}}{\sqrt{\pi}} \qquad \rho \geqq 0. \quad (20)$$

To apply the normalized impulse response (20) as plotted in Fig. 2 to a specific case, the β is calculated from (15) or (16) using physical data. The horizontal scale is then multiplied by β and the vertical scale divided by β to obtain the impulse response $g(x+Tl)$ vs x.

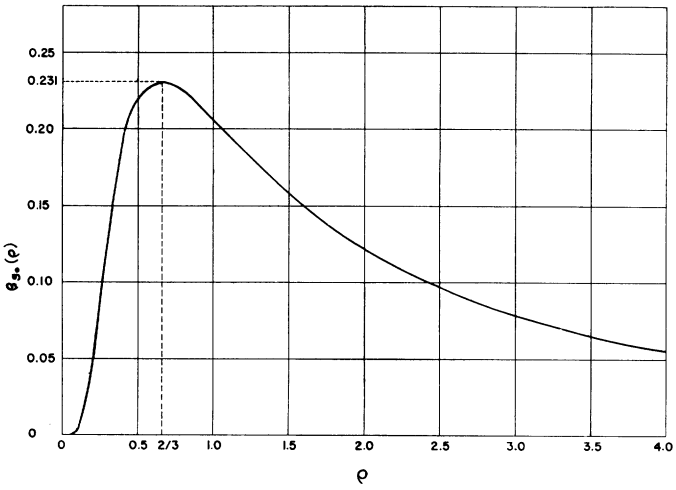

Fig. 2—Normalized impulse response,

$$\beta g(\rho) = \frac{\rho^{-1/\rho}\rho^{-3/2}}{\sqrt{\pi}}.$$

Performing the same transformation in (10), a normalized step response is obtained.

$$h_0(\rho) = \operatorname{cerf}\sqrt{\frac{1}{\rho}} \qquad \rho \geqq 0. \quad (21)$$

To obtain $h(x+Tl)$ vs x the horizontal scale is multiplied by the proper β.

Likewise, performing the same operation on (13), the normalized ramp response is obtained.

$$f_0(\rho) = \frac{1}{a'}\int_{\rho-a'}^{\rho}\operatorname{cerf}\sqrt{\frac{1}{\rho}}\,d\rho \qquad \rho \geqq 0 \quad (22)$$

where $a'=a/\beta$.

This represents a family of curves (Figs. 3, 4, and 5) with a' as the parameter. Practical utilization of them again requires only a time scale multiplication of magnitude β. Thus, the response of a particular piece of coaxial cable is obtained for a series of ramp inputs with 0–100 per cent rise times of $a'\beta$. For $a'=0$ the step re-

[6] This transformation is simple; however much confusion can arise if one does not state and visualize the problem. This is particularly true with respect to obtaining (22). See Appendix II for details.

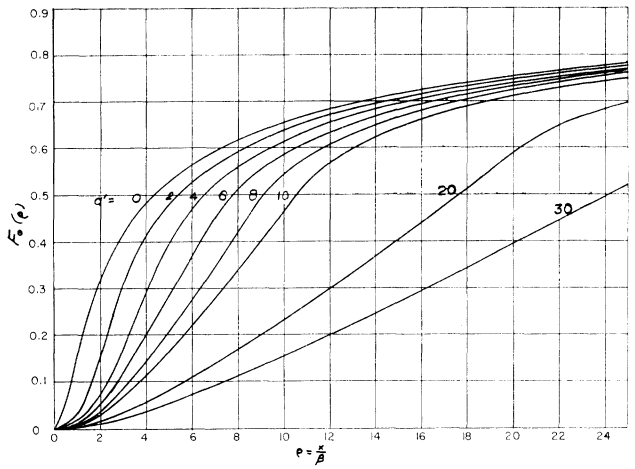

Fig. 3—Normalized ramp responses,

$$f_0(\rho) = \frac{1}{a'}\int_{\rho-a'}^{\rho} \operatorname{cerf}\sqrt{\frac{1}{\rho}}\,d\rho.$$

$$a' = \frac{a}{\beta}.$$

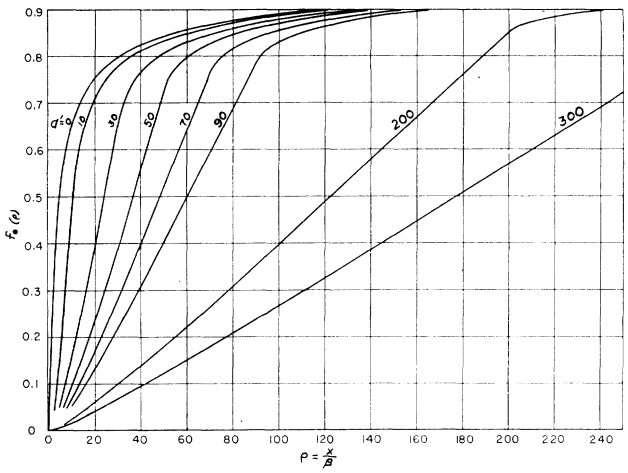

Fig. 4—Normalized ramp responses,

$$f_0(\rho) = \frac{1}{a'}\int_{\rho-a'}^{\rho} \operatorname{cerf}\sqrt{\frac{1}{\rho}}\,d\rho.$$

$$a' = \frac{a}{\beta}.$$

sponse (21) is obtained. The ramps corresponding to a' larger than the largest one plotted are relatively undistorted.

Experimental Verification

The experimental verification of the analysis which has been presented required the use of an extremely wide-band oscilloscope. Facilities which were available at the Naval Research Laboratory were used to obtain the transient response of eight pieces of coaxial cable.[7] Two time lengths of each of four types of cable, namely, RG-8/U, RG-58/AU, General Radio-874A2, and $\frac{7}{8}$-inch-diameter Styroflex, were tested. The signal applied to

[7] See Acknowledgment.

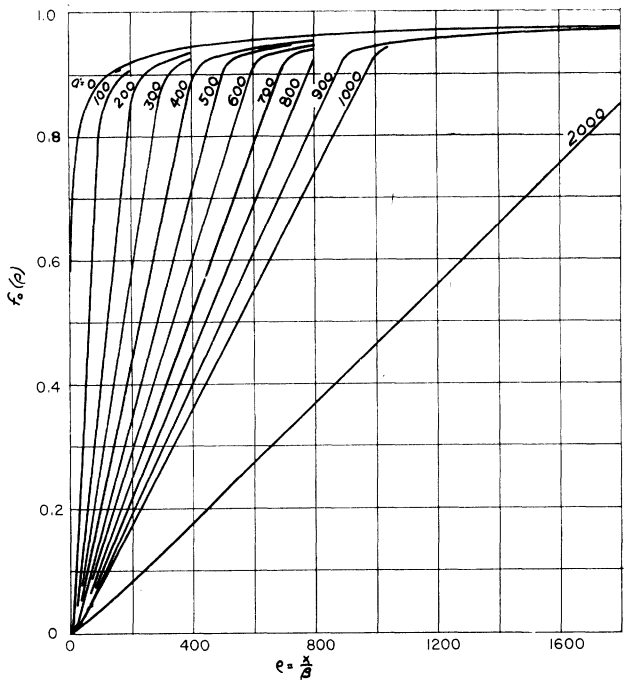

Fig. 5—Normalized ramp responses,

$$f_0(\rho) = \frac{1}{a'}\int_{\rho-a'}^{\rho} \operatorname{cerf}\sqrt{\frac{1}{\rho}}\,d\rho.$$

$$a' = \frac{a}{\beta}.$$

the cables was approximated by five ramp functions, and the response was calculated and compared with the observed response for each case.

Experimental System

Fig. 6 shows the cable comparison test circuit employing the NRL TW-10 traveling-wave cathode-ray tubes as the indicating instrument. The TW-10 has a bandwidth well in excess of 2000 mc, which should be sufficient for displaying rise times of the order of 0.1 mμs.

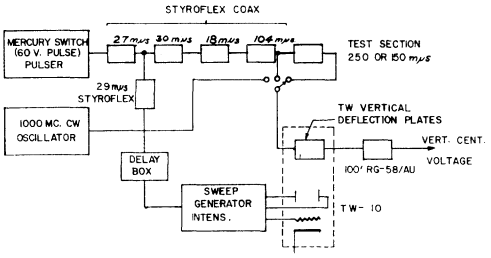

Fig. 6—Cable comparison test circuit.

The test pulse was generated by a mercury contact relay pulser giving a 60-volt pulse, 45 mμs wide and having a rise time of 0.25 mμs. Some signal delay (179 mμs of $\frac{7}{8}$-inch Styroflex) was required to allow time for operation of the sweep and intensifier circuits of the crt. The pulse observed at the end of the 179-mμs delay was called the standard pulse. Cable test sections of either 150 or 250 mμs were added, and the response

of the added sections to the standard pulse, as well as the standard pulse itself, were recorded photographically. Time reference was added to each photograph by applying a 1000-mc sine wave to the crt and taking double exposures.

Analysis of Data

Data was taken from the photographs using the sine wave as the time reference and the maximum amplitude of the standard pulse as the amplitude reference.

The rise of the standard pulse (Fig. 7) was approximated by five straight line-segments as specified in the following Table I.

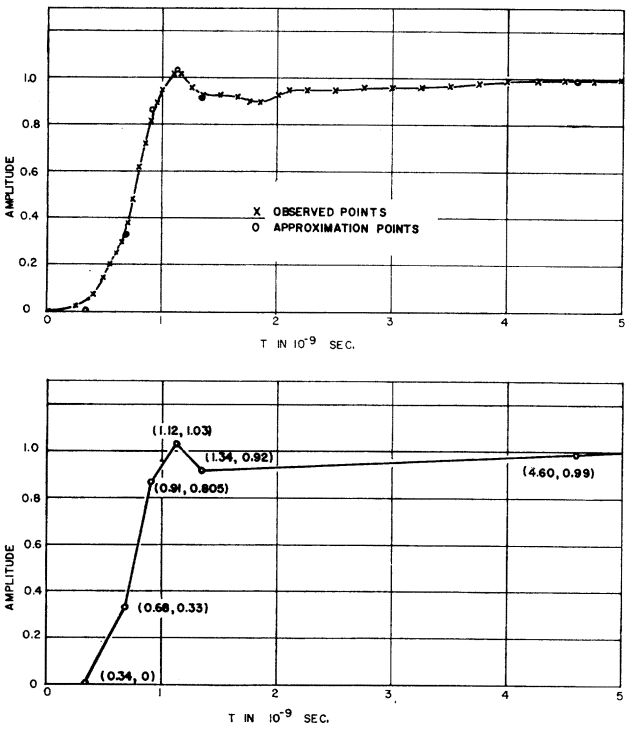

Fig. 7—Standard pulse and linear approximation.

The approximation to the standard pulse is then a succession of ramp functions having rise times and amplitudes as specified above and each starting at the appropriate t_0.

The β and appropriate values for a' for each case were calculated from (16) and $a'=a/\beta$ [see (22)]. Considering now each example (*i.e.*, 150-mμs delay of $\frac{7}{8}$-inch Styroflex), five ramp responses, one for each approximation segment, were calculated from the general curves in Figs. 3, 4, and 5.

The general curves consider ramp responses for ramps of amplitude unity; therefore, it was necessary to correct the amplitudes as listed in Table I. Points (in time) for calculation were preselected so that when the ramp responses were shifted according to the correct t_0 (listed in Table I) addition of ordinates would give the response to the standard pulse. The calculated responses as compared to the observed responses are given in Figs. 8–11 (next page).

In all cases no attempt was made to keep track of the zero time position of the transients. No information as to the time at which the transient first departed from zero amplitude after passing through a test section with respect to the time at which the transient "entered" the test section could be obtained. This difficulty is the same as is always met in relating physical transient data to mathematical prediction. The mathematician can define exactly a time before which the system is quiescent. However, the engineer must define the beginning of a transient as the time at which the waveform reaches same measurable value.

For comparison of calculation and observation, therefore, the curves were shifted in time relative to each other so the leading edges most nearly coincided at the region of steepest slope.

Experimental Results and Departures from Theory

From the comparisons of Figs. 8–11, one may conclude that in the coaxial cables considered the major cause of distortion of fact rise time transients is the skin effect. Each type of cable seems to have its own characteristic departure from the predicted response. During this study the causes of some of the departure has become apparent.

First, the analysis involves an approximation in taking the inverse transform of the transfer function as expressed in the validity constant A (7). The A for each case is indicated on the graphs (Figs. 8–11). As yet no quantitative measure has been developed to determine limits of error due to a particular value of A. However, the values of A in the examples considered are believed to be sufficiently small as to cause negligible error in the time range plotted. One may note that in the propagation constant $\gamma(p)$ (6) the first term ignored is a con-

TABLE I
Analysis of Standard Pulse

Line Segment	End Points of Segments (10^{-9} second, Amplitude)	Amplitude	0–100 Per Cent Rise Time	t_0
1	(0.34, 0); (0.68, 0.33)	0.330	0.34×10^{-9} second	0
2	(0.68, 0.33); (0.91, 0.805)	0.535	0.23	0.34×10^{-9} second
3	(0.91, 0.805); (1.12, 1.03)	0.165	0.21	0.57
4	(1.12, 1.03); (1.34, 0.92)	−0.110	0.22	0.78
5	(1.34, 0.92); (5.00, 1.00)	0.080	3.66	1.00

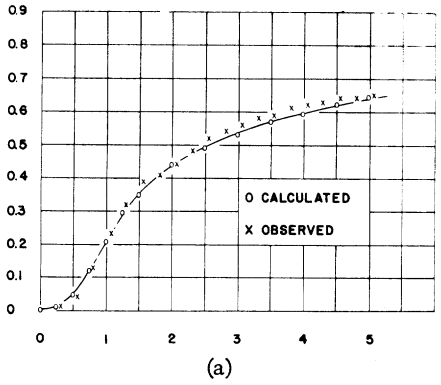

(a)

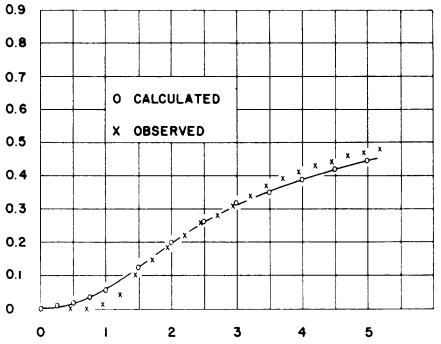

(b)

Fig. 8—Response of RG—58 A/u; A (100 mc) = 00.56.
(a) 150 mμs of cable—$\beta = 4.50 \times 10^{-10}$ second.
(b) 250 mμs of cable—$\beta = 1.25 \times 10^{-9}$ second.

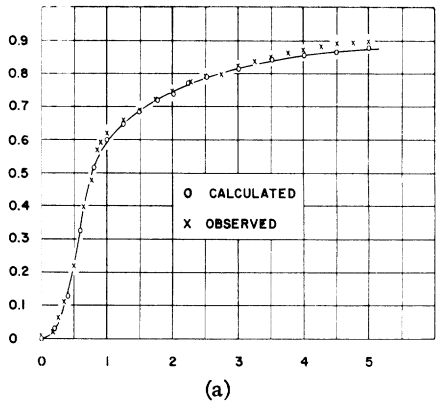

(a)

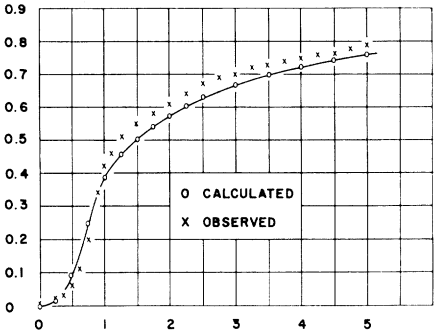

(b)

Fig. 10—Response of RG—8/u. A (100 mc) = 0.0024.
(a) 150 mμs of cable—$\beta = 8.14 \times 10^{-11}$ second.
(b) 250 mμs of cable—$\beta = 2.26 \times 10^{-10}$ second.

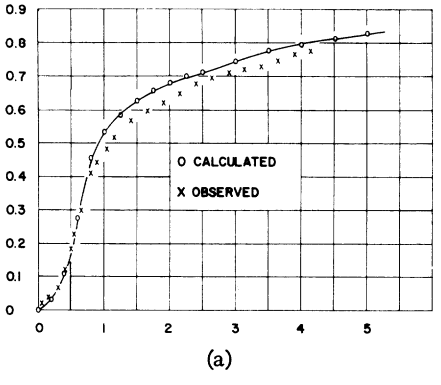

(a)

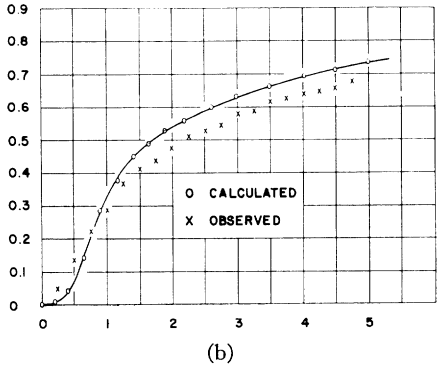

(b)

Fig. 9—Response of GR—874A2. A (100 mc) = 0.0027.
(a) 150 mμs of cable—$\beta = 1.02 \times 10^{-10}$ second.
(b) 250 mμs of cable—$\beta = 2.83 \times 10^{-10}$ second.

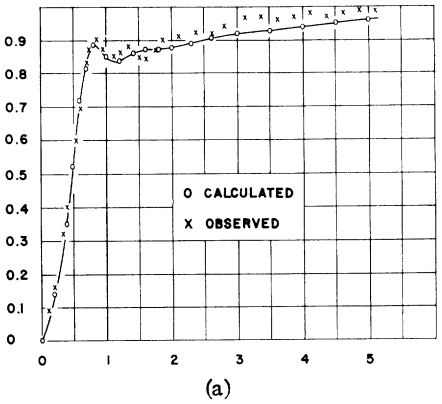

(a)

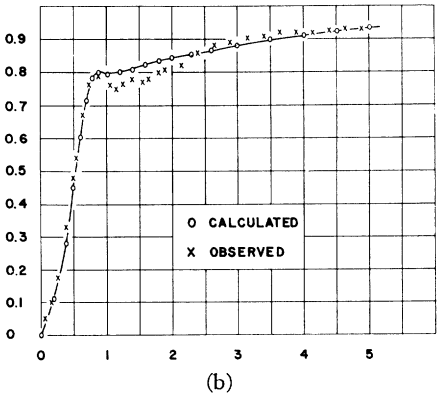

(b)

Fig. 11—Response of $\frac{7}{8}$ inch Styroflex. A (100 mc) = 0.00057.
(a) 150 mμs of cable—$\beta = 4.57 \times 10^{-12}$ second.
(b) 250 mμs of cable—$\beta = 1.27 \times 10^{-11}$ second.

stant (p^0 term) which adds nothing to the distortion and only insignificantly affects the amplitude.

The analysis assumes a $f^{0.5}$ law for the variation of attenuation with frequency [see (3) and (4)]. This is very nearly true for Styroflex cable. However, other cables have a somewhat greater exponent, GR-874 being as high as 0.6. A more elaborate analysis using f^m, $0 \leqq m \leqq 0.5$, has been made; however its usefulness is questionable since it cannot be directly related to the real physical problem. A realistic approach is to search for a second distorting factor such as dielectric loss which in this study was assumed to be negligible. Dielectric loss should be greater for GR-874 and other polyethylene dielectric cables than for Styroflex, although still it should not be the major distorting mechanism. Work on this phase of the problem is continuing.

Useful engineering results may be obtained even though the $f^{0.5}$ law is not followed exactly by the cable. The choice of the frequency at which β is evaluated (16) then becomes important. The frequency chosen in this study was $f_0 = 1000$ mc because the components of most importance were in the region of 1000 mc (considering a logarithmic frequency scale).

The bandwidth of the TW-10 was considered to be sufficient not to distort appreciably the response. The 10–90 per cent rise time of the standard pulse is 0.5 mμs. Approximately 700–900 mc of bandwidth (to the 3-db points) is needed to pass such a rise. The designers of the TW-10 oscilloscope system have established that the 3-db point of the deflection structure is well in excess of 2000 mc although no detailed data of deflection as a function of frequency is available. The ringing which is evident in some of the responses is probably due to the slight impedance discontinuities in the system.

Another possible source of error is in the nonlinearity of the crt deflection as a function of input amplitude. Checking this possibility showed that the crt deflection was within approximately 2 per cent of being linear. A slight curvature of the field of view (sometimes called "pin-cushion effect") made transcription of amplitude data difficult for time values of 3 to 5 mμs after the beginning of each response. Errors of up to 4 per cent (positive) may arise from this cause.

The RG-8 flexible connection between the TW-10 and the waveform to be observed (not explicitly shown in Fig. 6) does introduce appreciable distortion in the crt display; however, it does not invalidate the technique used to check the analysis.

Referring to Fig. 6, let the waveform entering the test section be represented by $F_1(p)$.[8] Let the transfer function of the 15-mμs RG-8 connecting cable be $G_1(p)$. Also let $F_1'(p)$ represent the waveform observed on the CRT (the standard pulse) when the test section is not included. Then, $F_1'(p) = F_1(p)G_1(p)$. Now let $G_2(p)$ be the transfer function of the test section of cable. Then, $F_2(p)$ which represents the waveform observed on the CRT when the test section is included is given by

$$F_2(p) = F_1(p)G_2(p)G_1(p)$$
$$= F_1(p)G_1(p)G_2(p) = F_1'(p)G(p)$$

since transfer functions of passive networks are commutative.

In words, what this means is that the distorting element, $G_1(p)$ having been present both in observation of the input and output of the test section allows isolation of the characteristics of the test section alone. This is the basis for all comparison type measurement techniques. For accuracy, the distortion due to $G_1(p)$ must be of the same order of magnitude or preferably less than that due to $G_2(p)$. It is less in all cases.

Conclusion

The analysis as described is a first order theory for the transient response of coaxial cables. As presented, it is useful in engineering problems involving millimicrosecond transients, however, later refinements in the theory may permit greater accuracy for cables in which dielectric loss is an appreciable factor.

Appendix I

The following identity was useful in the analysis.

$$I(x) \equiv \int_0^x \sqrt{\frac{\beta}{\pi}}\, \tau^{-3/2} e^{-\beta/\tau} d\tau = \operatorname{cerf} \sqrt{\frac{\beta}{x}}\,.$$

It may be verified by using Laplace Transformation operational theorems.[9] Letting L indicate the operation of taking the Laplace Transform and L^{-1} the inverse,

$$L[I(x)] = \frac{1}{p} L\left[\sqrt{\frac{\beta}{x}}\, x^{-3/2} e^{-\beta/x}\right] = \frac{1}{p} e^{-2\sqrt{\beta p}}$$

$$I(x) = L^{-1}L[I(x)] = L^{-1}\left[\frac{1}{p} e^{-2\sqrt{\beta p}}\right] = \operatorname{cerf} \sqrt{\frac{\beta}{x}}.$$

This inverse has been listed.[5]

Since a function which is expressed as a definite integral with a variable in the limits is a function only of the limits, then

$$I(x - a) = \int_0^{x-a} \sqrt{\frac{\beta}{\pi}}\, \tau^{-3/2} e^{-\beta/\tau} d\tau = \operatorname{cerf} \sqrt{\frac{\beta}{x - a}}.$$

Appendix II

The normalization of (9), (10), and (13) to obtain (19), (21), and (22) is performed as follows. Consider first (9) and (10).

$$g(x + Tl) = \sqrt{\frac{\beta}{\pi}}\, x^{-3/2} e^{-\beta/x} \qquad x \geqq 0 \qquad (9)$$

$$h(x + Tl) = \operatorname{cerf} \sqrt{\frac{\beta}{x}} \qquad x \geqq 0. \qquad (10)$$

[8] These expressions are given in complex variable form as Laplace transforms of the time functions.

[9] C. R. Wylie, "Advanced Engineering Mathematics," McGraw-Hill Book Co., Inc., New York, N. Y.; 1951.

Let $x=\beta\rho$

$$g(\beta\rho + Tl) = \sqrt{\frac{\beta}{\pi}}(\beta\rho)^{-3/2}e^{-1/\rho} = \frac{\rho^{-3/2}e^{-1/\rho}}{\beta\sqrt{\pi}}$$

$$h(\beta\rho + Tl) = \text{cerf}\sqrt{\frac{1}{\rho}}.$$

As written above, the functions g and h are still plotted on the x time scale although x does not appear in the expressions. Changing the time scale to the dimensionless ρ (β has the dimensions of time) new functions $g_0(\rho)$ and $h_0(\rho)$ are obtained.

$$g_0(\rho) = \frac{\rho^{-3/2}e^{-1/\rho}}{\beta\sqrt{\pi}} \qquad \rho \geqq 0 \qquad (19)$$

$$h_0(\rho) = \text{cerf}\sqrt{\frac{1}{\rho}} \qquad \rho \geqq 0. \qquad (21)$$

For plotting, (19) is changed to

$$\beta g_0(\rho) = \frac{\rho^{-3/2}e^{-1/\rho}}{\sqrt{\pi}} \qquad \rho \geqq 0. \qquad (20)$$

Note that in the transformation the shape of the functions were preserved, and in order to plot the functions $g(x+Tl)$ and $h(x+Tl)$ for any particular physical case the horizontal scale is altered by the factor β for that case. In (20) the vertical scale must also be altered by the factor β.

Considering (13), more care must be used in the change of time scales.

$$f(x + Tl) = \frac{1}{a}\int_{x-a}^{x} \text{cerf}\sqrt{\frac{\beta}{\tau}}\,d\tau \qquad x \geqq 0. \qquad (13)$$

In the above, change the scale on the dummy variable by the substitution $t=\beta\rho$. A corresponding change of scale must be made in the limits by dividing by β

$$f(x + Tl) = \frac{1}{a}\int_{(x-a)/\beta}^{x/\beta} \text{cerf}\sqrt{\frac{1}{\rho}}\,\beta d\rho.$$

The function is now set up for normalization by letting $x=\beta\rho$ and plotting the resulting function $f_0(\rho)\equiv f(\beta\rho+Tl)$ vs ρ

$$f_0(\rho) = f(\beta\rho + Tl) = \frac{\beta}{a}\int_{(\beta\rho-a)/\beta}^{\beta\rho/\beta} \text{cerf}\sqrt{\frac{1}{\rho}}\,d\rho.$$

Finally, letting $a'=a/\beta$,

$$f_0(\rho) = \frac{1}{a'}\int_{\rho-a'}^{\rho} \text{cerf}\sqrt{\frac{1}{\rho}}\,d\rho \qquad \rho \geqq 0. \qquad (22)$$

Acknowledgment

The cooperation of the Naval Research Laboratory, specifically, the group under G. F. Wall, was vital in securing the experimental data. The experiment was set up and the photographs were taken by them. Also, the same analytical conclusions concerning the role of skin effect in coaxial cables have been reached independently by R. V. Talbot, F. E. Huggin, and C. B. Dobbie of NRL.

Others who have contributed significant amounts are G. W. Kimball of the Department of Defense, who supplied the rigorous mathematical steps to verify (22) which had originally been deduced by physical reasoning and E. D. Reilly of the Department of Defense who did the computer programming for the calculation of the curves in Fig. 3, 4, and 5. Drafting for the figures was done by Paul Peters and Cletus Isbell of the University of Kansas.

CORRECTION

The editors wish to point out the following correction to "SSB Performance as a Function of Carrier Strength," by William L. Firestone, which appeared on pages 1839–1848 of the December, 1956 issue of PROCEEDINGS. On page 1843, the illustrations in the first column identified as Fig. 10 and Fig. 11 should be transposed.